

Effect of Normal Force Dispersion on the Mobility of Wheeled Robots Operating on Soft Soil

Bahareh Ghotbi, Francisco González, József Kövecses and Jorge Angeles

Abstract—A number of applications of wheeled robots, including planetary exploration rovers and rescue missions, require that the vehicle operates in a non-structured environment. Optimizing the vehicle mobility is of key importance in such applications. Reduced mobility can limit the ability of the robot to achieve the mission goals, or even render it immobile in extreme cases. In this paper, the effect of normal contact forces on mobility is reported. A performance indicator based on the force distribution is defined and used to compare different vehicle configurations. The validity of this indicator was assessed using both simulation and experimental results obtained for a six-wheel rover prototype. Results suggest that modifying the robot configuration to alter the normal force distribution can lead to increased traction force available at the wheel-terrain interfaces, thus improving the mobility.

I. INTRODUCTION

Optimizing the vehicle mobility is an important goal in the design and operation of wheeled robots on soft soil. However, mobility can be defined in several ways in the context of such systems, and there is no general agreement in the literature about the precise meaning of this term. For wheeled robots, mobility can be understood in the sense of the ability to move from a certain configuration, or to move with maximum speed. This definition is close to the *trafficability* concept introduced in [1], which points to the capacity of the vehicle to overcome terrain resistance and generate traction.

There is also a lack of consensus regarding which strategies are the best to enhance the mobility of wheeled robots operating on unstructured terrain. Reduction of the slip at the wheel-terrain contact area has been proposed as a way to achieve this objective [2], [3]. In these papers, the wheel-terrain interface is modeled using the assumption of Coulomb friction and the ratio of tangential to normal forces at the wheel-ground contact is minimized with the goal of reducing the risk of developing slip. While not directly dealing with soft soil modeling, these papers highlight the need for keeping wheel slip under control in order to improve mobility.

When soft terrain enters the picture, the phenomena at the wheel-terrain interface become more complex and Coulomb friction models can no longer be used to describe them accurately. Then, two options are left in order to predict the effect of design and actuation parameters on robot mobility.

Authors are with the Department of Mechanical Engineering and the Centre for Intelligent Machines, McGill University, Montreal, Quebec H3A 0C3, Canada. bahareh.ghotbi@mail.mcgill.ca, franglez@cim.mcgill.ca, jozsef.kovecses@mcgill.ca, angeles@cim.mcgill.ca

The first one is turning to detailed, realistic models of the contact interface. These models are typically used in forward-dynamics simulation settings and require the accurate knowledge of a set of parameters that are not always easy to determine. The second option consists in finding design and operation guidelines of general validity. Even when these do not provide exact numerical values, they offer simple means to compare alternative designs and can be used to define objective functions for design, operation, and control.

The effect of the normal force distribution on mobility on soft soil has been mentioned several times in the literature. Based on results obtained from experiments with a four-wheel rover, it is stated in [4] that a variation in the normal force distribution does not change the sum of traction forces for the vehicle considered as a whole. It is acknowledged in the same work, though, that a balanced load distribution helps reducing the resistant torque on some wheels, thus improving the rover mobility.

On the other hand, some researchers mention a uniform distribution of normal forces among the factors that enhance mobility. In [5], the authors state that balancing the normal loads helps the vehicle to develop a higher value of the overall traction force. Along the same lines, it is suggested in [6] that uniformly distributing the weight of the rover among the wheels is a valid strategy to achieve better mobility, when not enough information about contact forces is available. A similar conclusion can be found in [7]: the load repartition among the wheels has to be even on flat ground to achieve the best performance. As a consequence, special attention must be paid to good adaptation to the terrain and the position of the center of mass when deciding on the structure of the rover. Work reported in [8] is an experimental confirmation of these statements for a particular rover design.

The level of slip must be considered together with the terrain reaction forces when studying mobility. According to the drawbar pull-slip curve, net traction force can be increased by allowing a higher slip value to develop (e.g. via applying a greater driving torque to the wheels) [9]. However, if the slip ratio goes beyond a certain value, then the drawbar pull goes down. The concepts of traction margin and slip margin are thus defined for their use in traction control. The positive effect of uniform load distribution on the improvement of climbing ability is also mentioned in [9]. In the tests reported by [10], the engineering model of Spirit and Opportunity was placed on a variable terrain tilt platform to measure the climbing ability for different slip ratios. It was found that the slip-drawbar pull curve is highly non-linear and up to 91% of slip was observed for climbing a 20° slope

on soft soil.

Despite being mentioned in a significant number of references as a factor to take into account when evaluating mobility, normal force distribution has not yet been studied in a systematic way with regard to its role in traction. The purpose of the current paper is to determine whether in fact a balanced normal load distribution improves the traction developed by a wheeled robot and, if so, to what extent. A general framework, not limited to the study of a specific vehicle design or type of terrain, was adopted to ensure the general validity of the results.

II. METHODOLOGY

The interaction between a rigid wheel and soft soil under steady-state conditions is commonly modeled using terramechanics relations [11]. Following this approach, the forces at the wheel-terrain interface (Fig. 1) can be obtained as functions of the state of the vehicle, the angular and translational velocities of the wheels, and a set of parameters that define the nature of the terrain.

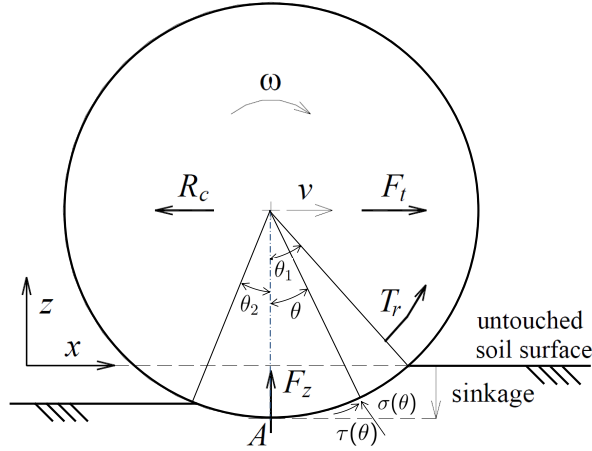


Fig. 1. Terrain reactions on a driven single wheel on soft soil

The normal stress at the wheel-terrain interface is given by [11]:

$$\sigma(z) = \left(\frac{k_c}{b} + k_\phi \right) z^n \quad (1)$$

where b is the wheel width, n is the sinkage exponent, and k_c and k_ϕ are the pressure-sinkage moduli associated with the soil cohesive and frictional components, respectively.

Shear stress can be determined as:

$$\tau(\theta) = (c + \sigma(\theta) \tan \phi) \left(1 - e^{\frac{r}{K_d} [\theta_1 - \theta - (1-i)(\sin \theta_1 - \sin \theta)]} \right) \quad (2)$$

where c is the terrain cohesion, ϕ is the internal friction angle, r is the wheel radius, K_d is the shear deformation modulus, and i is the wheel slip, defined as $i = (r\omega - v)/r\omega$.

If the above quantities are known, the values of the normal force (F_n) that each wheel bears and the drawbar pull (F_x =

$F_t - R_c$) it is capable to develop can be derived from the terramechanics expressions, namely,

$$F_x = rb \left(\int_{\theta_2}^{\theta_1} \tau(\theta) \cos \theta d\theta - \int_{\theta_2}^{\theta_1} \sigma(\theta) \sin \theta d\theta \right) \quad (3)$$

$$F_n = rb \left(\int_{\theta_2}^{\theta_1} \tau(\theta) \sin \theta + \int_{\theta_2}^{\theta_1} \sigma(\theta) \cos \theta d\theta \right) - c_z \dot{z} \quad (4)$$

where $c_z \dot{z}$ is a modification from the original form, as introduced in [12], where c_z is a damping coefficient and \dot{z} is the sinkage velocity in the vertical direction.

The effect of uneven normal forces can be studied using the F_x vs. F_n curve. An example for a three-axle system in 2-D motion is shown in Fig. 2.

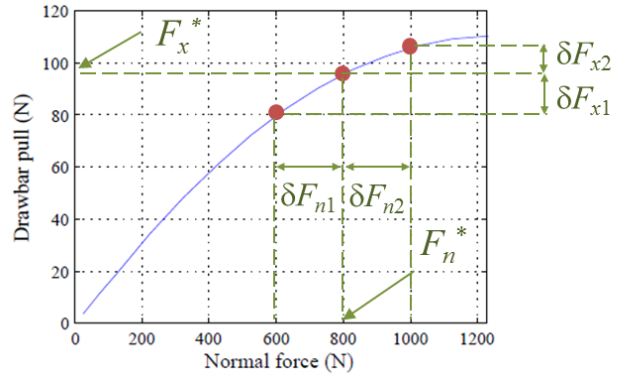


Fig. 2. Effect of non-uniform normal force distribution on the total available drawbar pull

If the three axles are moving with the same angular speed, and the terrain under the vehicle is homogeneous, then the same curve can be used for all the wheels. Multi-pass effect is not considered for the purposes of this work. In this case, a balanced distribution of normal forces would be the one in which $F_{n1} = F_{n2} = F_{n3} = F_n^*$. A transference of normal load between the first and second axles of the robot ($\delta F_{n1} = -\delta F_{n2}$) will result in changes δF_{x1} and δF_{x2} in the drawbar pull at these wheels. If the slope of the F_x vs. F_n curve is consistently decreasing, then $\delta F_{x2} < \delta F_{x1}$ and this will yield a lower total available drawbar pull for the same level of slip of the vehicle. In other words, the slip should become higher in order to achieve the same traction delivered by the balanced configuration.

The shape of the F_x vs. F_n curve varies with the percentage of slip the wheel is experiencing and also with the soil properties. Identifying the most influential factors and the conditions under which the relation becomes highly non-linear helps determine the range of conditions under which achieving a uniform normal load distribution will result in a significant mobility improvement. This study is outlined below.

A. Factors affecting the shape of the F_x vs. F_n curve

In order to determine the effect of slip and soil parameters on the relation between F_n and F_x , a virtual single-wheel

testbed was used. A set of simulations of the motion of a single wheel moving on soft terrain was carried out using terramechanics relations to model the wheel-terrain interaction. The wheel properties were chosen to match those of the rover prototype described in Section III. The wheel mass was $m = 2.55$ kg, its radius $r = 0.175$ m, and its width $b = 0.15$ m. The slip at the contact with the ground was specified by kinematically guiding the wheel, so both its angular velocity ω and the velocity of its center v were known. The normal force F_n representing the total load on the wheel-terrain interface was adjusted for each simulation run, in a range of up to 1000 N. Table I shows the baseline soil parameters used to draw the curves.

TABLE I

BASELINE SOIL PROPERTIES USED IN THE DETERMINATION OF THE F_x VS. F_n CURVES

n	c	ϕ	k_c	k_ϕ	K_d
-	[N/m ²]	[deg]	[N/m ^{$n+1$}]	[kN/m ^{$n+2$}]	[m]
1	220	33.1	1400	820	0.015

Moreover, different sets of curves were obtained by modifying the terrain properties. As illustration of the results, Figs. 3 and 4 display the plots obtained for two different values of the pressure-sinkage frictional modulus k_ϕ .

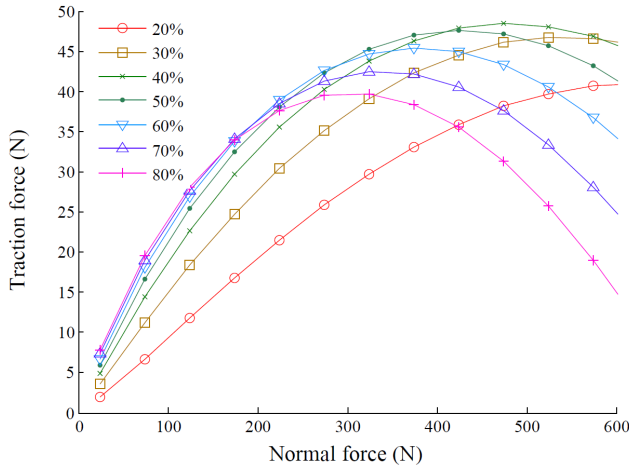


Fig. 3. Drawbar pull vs. normal load for a single wheel with different slip ratios and $k_\phi = 820$ kN/m ^{$n+2$}

The obtained plots reveal that the relation between F_n and F_x is practically linear for low values of F_n and slip. On the other hand, heavier normal loads on the wheel and values of the slip over 50 % bring along significant deviations from linearity. These are accentuated by low values of the k_ϕ modulus, which was found to be the most influential of all terrain parameters with regard to the curvature of the plot. The shear modulus K_d of the terrain has a significant effect too, as lower values of this parameter result in a steeper curve.

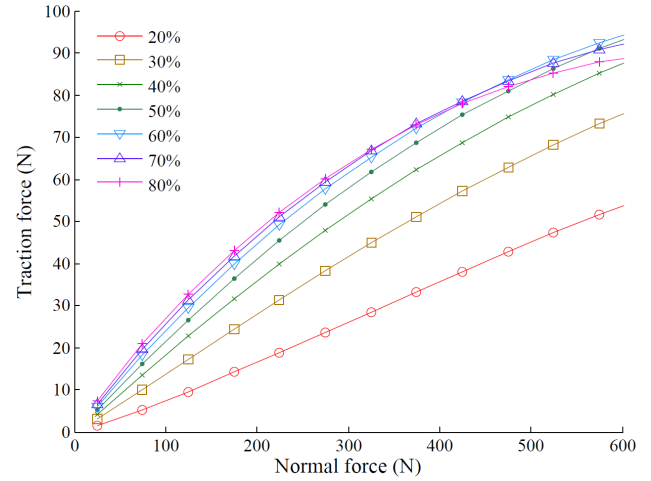


Fig. 4. Drawbar pull vs. normal load for a single wheel with different slip ratios and $k_\phi = 2000$ kN/m ^{$n+2$}

As a conclusion, it can be stated that making the normal force distribution more uniform will have a noticeable effect on net traction when the F_x vs. F_n plot exhibits high curvature values. This is the case of operation conditions where high values of the slip are expected to develop, such as slope climbing, or in the presence of loose terrain with low values of k_ϕ . In other situations, with an almost linear F_x vs. F_n plot, such as when moving on flat ground or climbing mild slopes on cohesive terrain, the uniformity of the normal load distribution will still have a positive effect on rover mobility, but this may not be significant.

B. Definition of the performance indicator

For the case of a wheeled robot operating on homogeneous terrain, the F_x vs. F_n relation will be the same for all the wheels if they are identical and the slip under each wheel is the same. These assumptions can be considered close enough to reality in a wide variety of operation conditions.

The *Normal Force Dispersion* (η) is introduced here as a measure of the uniformity of the normal load distribution. This performance indicator is defined based on the standard deviation of the normal forces F_n at the wheel-terrain contact interfaces as

$$\eta(F_{n1}, \dots, F_{np}) = \sqrt{\frac{1}{p} \sum_{i=1}^p (F_{ni} - \mu)^2} \quad (5)$$

where p is the number of wheels of the vehicle and

$$\mu = \frac{1}{p} \sum_{i=1}^p F_{ni} \quad (6)$$

A totally balanced distribution of normal forces ($F_{n1} = F_{n2} = \dots = F_{np}$) results in $\eta = 0$.

The main application of this indicator is in the assessment and comparison of several configurations of the same vehicle on a determined type of soil. It can be used as a tool to determine which configuration produces the most uniform load distribution among the wheels.

III. CASE STUDY

The performance indicator described in Section II-B was used in the study of the Rover Chassis Prototype (RCP), a six-wheel rover prototype developed by MDA Space Missions (Fig. 5).

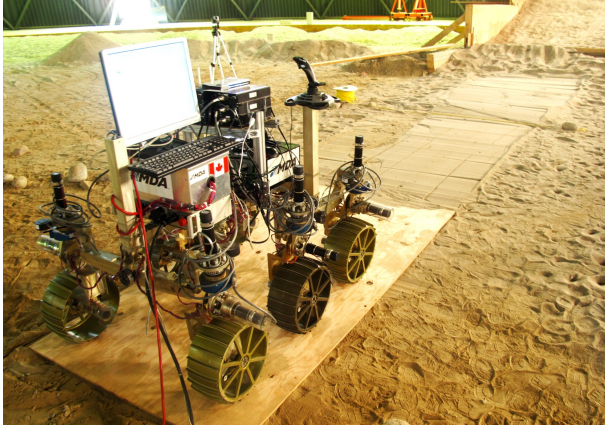


Fig. 5. The RCP rover

A set of experiments, including drawbar-pull tests with variable loads and wheel slip (Fig. 6), was carried out on soft, sandy soil with unknown properties. A set of weights (22.5 kg) was placed in different locations on the vehicle chassis in order to obtain various distributions of the normal loads at the wheels. The force measurements from both the force/torque sensors mounted on each leg of the rover and a load cell attached to the rope used during the drawbar pull tests were recorded, as well as the readings from encoders at each wheel. The rover was operated under velocity control. All the wheels were commanded to move with the same angular velocity. The forward velocity of the rover was measured using a system of visual references. This resulted in a set of experimental data that comprised the drawbar pull and the slip corresponding to each experiment.



Fig. 6. Drawbar pull test with the RCP

Next, a model of the rover (Fig. 7) was built using a multibody software tool developed by the authors [13], implemented in MATLAB.

Each experiment was reproduced in a forward-dynamics simulation setting with this code, using the terramechanics relations described in [11] to model the wheel-soil inter-

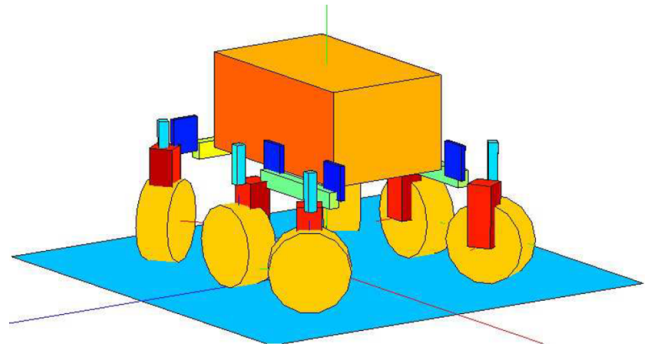


Fig. 7. Multibody model of the RCP

action. These simulations were used to identify the soil parameters.

A. Soil parameter identification

The process of tuning the soil parameters included running a forward-dynamics simulation for each of the 15 test cases using a single set of soil parameters. The effect of the variation of each soil parameter on the obtained drawbar pull-slip curve and the wheel sinkage was studied. It was observed that the most influential parameters in the range of the weight and operation of the RCP are k_ϕ , which affects the sinkage value, and K_d , which modifies the shape of the drawbar pull-slip curve. It can be seen from eq. (1) that for a certain load applied on the wheel, a higher value of k_ϕ results in a smaller wheel sinkage. Also, in eq. (2) the relation between shear stress and normal stress includes an exponential term. This exponential term itself is a function of the slip ratio and the shear deformation modulus, which suggests that smaller values of K_d result in a steeper slope of the curve.

TABLE II
SOIL PROPERTIES OBTAINED AFTER TERRAIN PARAMETER IDENTIFICATION

n	c	ϕ	k_c	k_ϕ	K_d
-	[N/m ²]	[deg]	[N/m ⁿ⁺¹]	[kN/m ⁿ⁺²]	[m]
1	220	33.1	1400	2000	0.015

The internal friction angle ϕ was estimated during the experiments. A box was slowly filled with the sand on which the rover operated in order to form a small heap. The angle of the heap was measured, which gave an estimation of the internal friction angle of the soil, ϕ . Figure 8 shows that with the tuned soil parameters from Table II the simulation results and experimental data show a quite reasonable match.

The sinkage value of the wheels in the simulation results was 0.02 m, which matched the experimentally obtained data as well.

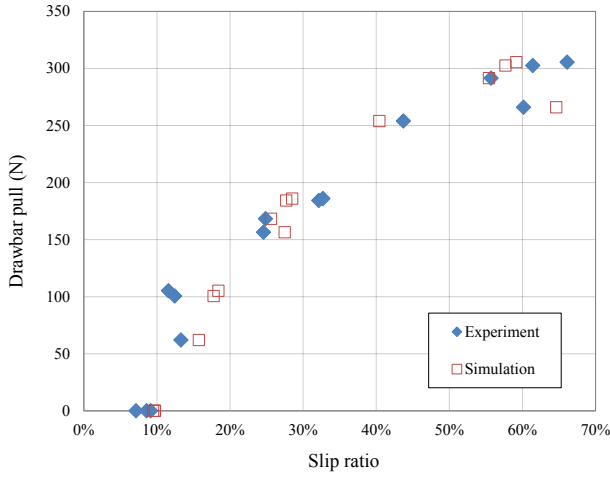


Fig. 8. Match between experimental measurements and simulation results for the tuned set of soil parameters (Table II)

B. Effect of normal force distribution

The multibody model and code were used to predict the effect of the uniformity of the normal load distribution on the drawbar pull the vehicle can develop for a given value of the slip ratio. Two samples from the set of experiments with different mass distribution were selected to this end, and the value of η was determined for each case. The wheels of the rover were commanded to move with a constant angular speed $\omega = 0.4$ rad/s and a different external load was applied to the body of the rover in each experiment, which resulted in two different values for the slip.

Next, forward-dynamics simulations of the selected cases were carried out using the multibody code. The RCP model was kinematically guided to move with the values of ω and v corresponding to each case, ensuring that the slip was the same in simulations and experiments. Terramechanics relations were used with the soil parameters in Table II to evaluate the terrain reactions. The drawbar pull predicted by simulation was in agreement with the sensor measurements.

TABLE III

EFFECT OF A MORE UNIFORM LOAD DISTRIBUTION ON THE DRAWBAR PULL OF RCP

Case	Slip [-]	η [N]	F_x [N]		η^* [N]	F_x^* [N]
			Sim.	Exp.		
1	55 %	12	301.1	292.0	0.02	301.2
2	43 %	36	266.9	254.0	0.02	267.7

The effect of uniform normal load distribution was assessed readjusting the mass configuration of the model to obtain a value of η close to zero (η^*). A new simulation was run for each case, keeping constant the values of ω , v , and consequently the slip. The value of the drawbar pull with the more even load distribution (F_x^*) is shown in Table III. The slip ratio in cases 1 and 2 differs. Therefore, the two cases

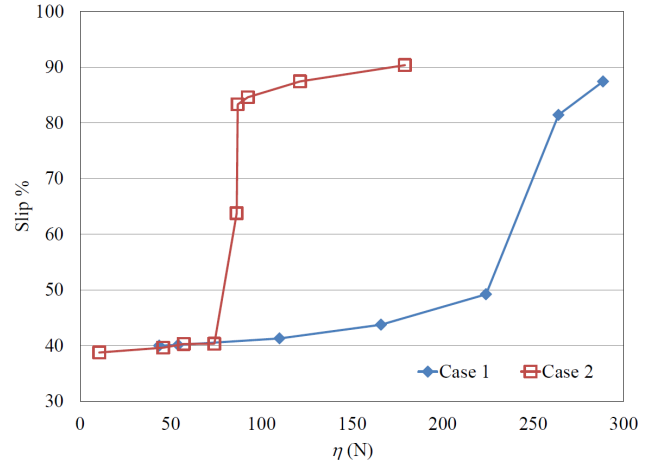


Fig. 9. Values of the slip vs. η index developed by RCP while climbing two different slopes: 10° with $k_\phi = 2000$ kN/mⁿ⁺² (case 1), and 8.7° with $k_\phi = 820$ kN/mⁿ⁺² (case 2), for an extra load of 22.5 kg

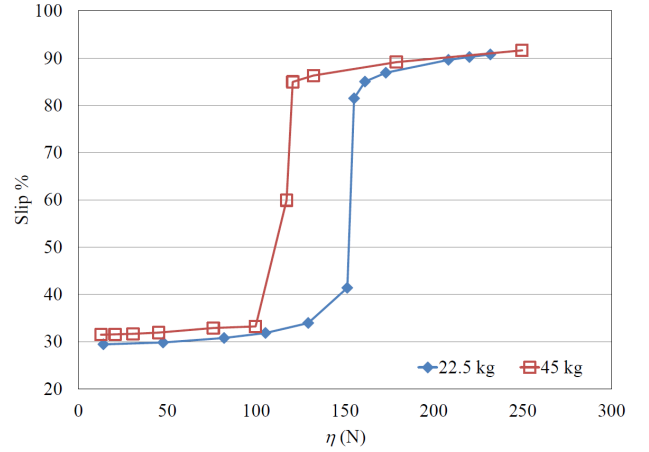


Fig. 10. Values of the slip vs. η index developed by RCP while climbing a 7.5° slope on soft terrain, for two different values of the extra load on the rover

are not comparable in terms of the effect of their Normal Force Dispersion on the value of the drawbar pull the vehicle develops. However, by comparing each case independently it can be seen that a uniform normal force distribution actually increases the value of the drawbar pull that the vehicle can develop. Nevertheless, the increase is small and does not have a significant effect on mobility. This is in agreement with the discussion in Section II-A. The F_x vs. F_n curve for the terrain on which the rover operated during the experiments is comparable to Fig. 4. Given the values of the slip (between 40 and 60 %) and the normal load per wheel (between 100 and 350 N), it becomes apparent that the operation point of the rover is located in an almost linear region of the F_x vs. F_n diagram.

In order to study the effect of normal load dispersion in the highly non-linear region of the diagram, a new set of simulations was performed. First, the effect of soil parameter k_ϕ was studied with a set of simulations. The model of the RCP was commanded to climb a slope with

the set of additional masses of 22.5 kg. The maneuver was simulated for two different scenarios. First, the maneuver on a 10° slope with the soil properties summarized in Table II was considered again. Next, the pressure-sinkage frictional modulus (k_ϕ) of the soil was decreased to 820 kN/mⁿ⁺² and the motion of the RCP was simulated for different values of η . This modification in the soil properties produced higher sinkage of the wheels and resulted in values for the slip close to 90% even for low values of η .

In order to make the two scenarios comparable, the slope angle was reduced until the rover configuration with a more even mass distribution, i.e. small η , reaches the same value of slip on both types of soil considered here. Results are shown in Fig. 9. The comparison of the two cases showed that for $\eta \leq 80$ the percentage of slip was similar in both scenarios. However, the terrain with low k_ϕ was not able to provide enough traction for values of η beyond this point, which resulted in slip percentages close to 90%. On the other hand, the RCP was able to climb the slope on the original terrain (Table II) even with more severe dispersions of normal forces, while keeping slip under 50%. This observation agrees with the changes in the shape of the F_x vs. F_n curve due to the variation of k_ϕ , as discussed in Section II-A, and confirms that the rover ability to climb a slope is more sensitive to load dispersion on terrain with smaller values of k_ϕ .

The highly non-linear region of the F_x vs. F_n diagram can also be reached by increasing the normal load on the wheels. A new set of simulations was performed with two values of the total payload on the rover. The chosen terrain properties were the ones in Table I because, as mentioned above, a rover operating on a terrain with low k_ϕ is more likely to experience mobility issues. The two values of the extra weight added to the rover chassis were 22.5 and 45 kg, and the value of η was modified by regulating its location relative to the center of mass of the body of the vehicle. The simulation represented the RCP climbing a slope of 7.5°. Results are summarized in Fig. 10. Both cases behave similarly for $\eta < 100$ N. Beyond this point, the rover with a 45 kg payload develops a wheel slip close to 90%, while the lighter one can climb the slope keeping the slip under 50% until η reaches 150 N.

The higher value of the extra mass increases the load F_n^* that each wheel would be carrying if the load were uniform. This displaces the operation point of the rover towards a more non-linear region of the F_x vs. F_n curve depicted in Fig. 4. In this situation, the effect of a greater η is more significant. A change in the load dispersion η will be more influential on the vehicle mobility in the highly non-linear region of the F_x vs. F_n curve. Consequently, in these cases making the normal force distribution more uniform will improve the mobility of the vehicle more considerably. Therefore, less slip will be developed at the wheel-terrain interface in order to obtain the necessary traction force to climb the slope.

IV. CONCLUSIONS

In this work, the effect of normal force distribution on mobility of wheeled robots was studied. A performance indicator that quantifies the dispersion of the normal force at the wheel-terrain interface was defined. This indicator can be used to enhance the mobility of a wheeled robot on soft soil, including slope negotiation maneuvers, for example via robot reconfiguration. The actual impact of the normal force distribution on the total available traction was found to depend on a set of factors. Experimental and simulation results with a multibody model of a six-wheeled rover showed that high values of wheel slip and normal force, and low values of k_ϕ amplify the effects of unbalancing the normal force distribution.

ACKNOWLEDGMENT

This research was supported by the Natural Sciences and Engineering Research Council of Canada, and MDA Space Missions. The support is gratefully acknowledged.

REFERENCES

- [1] D. Apostolopoulos, Analytic Configuration of Wheeled Robotic Locomotion, Ph.D. dissertation, Carnegie Mellon Univ., USA, 2001.
- [2] P. Lamon, A. Krebs, M. Lauria, R. Siegwart, and S. Shooter, Wheel Torque Control for a Rough Terrain Rover, in Proc. of the 2004 IEEE Int. Conf. on Robotics and Automation, New Orleans, LA (USA), 2004.
- [3] T. Thuerer, A. Krebs, R. Siegwart, and P. Lamon, Performance Comparison of Rough-Terrain Robots – Simulation and Hardware, Journal of Field Robotics, vol. 24 (3), pp. 251–271, 2007.
- [4] G. Ishigami, Terramechanics-based Analysis and Control for Lunar/Planetary Exploration Robots, Ph.D. dissertation, Dept. of Aerospace Engineering, Tohoku Univ., Japan, 2008.
- [5] C. Grand, F. BenAmar, F. Plumet, P. Bidaud, Stability and Traction Optimization of Reconfigurable Vehicles. Application to a Hybrid Wheel-Legged Robot, The Int. Journal of Robotics Research, vol. 23 (10-11), pp. 1041–1058, 2003.
- [6] G. Freitas, G. Gleizer, F. Lizarralde, L. Hsu, and N. R. Salvi dos Reis, Kinematic Reconfigurability Control for an Environmental Mobile Robot Operating in the Amazon Rain Forest, Journal of Field Robotics, vol. 27 (2), pp. 197–216, 2010.
- [7] S. Michaud, L. Richter, N. Patel, T. Thüer, T. Huelsing, L. Joudrier, R. Siegwart, and A. Ellery, RCET: Rover Chassis Evaluation Tools, in Proc. 8th ESA Workshop on Adv. Space Tech. for Robotics and Automation (ASTRA), Noordwijk (The Netherlands), 2004, paper O-01.
- [8] B. Ghotbi, F. González, J. Kövecses, and J. Angeles, Vehicle-Terrain Interaction Models for Analysis and Performance Evaluation of Wheeled Rovers, in Proc. 25th IEEE/RSJ Int. Conf. on Intelligent Robots and Systems (IROS), Vilamoura (Portugal), 2012, pp. 3138–3143.
- [9] K. Yoshida, T. Watanabe, N. Mizuno, and G. Ishigami, Terramechanics-Based Analysis and Traction Control of a Lunar/Planetary Rover, in S. Yuta et al. (Eds.): Field and Service Robotics, STAR 24, pp. 225234, Springer-Verlag, 2006.
- [10] R. A. Lindemann, C. J. Voorhees, Mars Exploration Rover Mobility Assembly Design, Test and Performance, in Proc. IEEE Int. Conf. on Systems, Man and Cybernetics, Waikoloa, HI (USA), 2005, pp.450–455.
- [11] J.Y. Wong, Theory of Ground Vehicles, John Wiley & Sons, Inc, 2008.
- [12] A. Azimi, M. Hirschkorn, B. Ghotbi, J. Kövecses, J. Angeles, P. Radziszewski, M. Teichmann, M. Courchesne, and Y. Gonthier, Terrain modelling in simulation-based performance evaluation of rovers, Canadian Aeronautics and Space Journal, vol. 57 (1), pp. 24-33, 2011.
- [13] B. Ghotbi, F. González, A. Azimi, W. Bird, J. Kövecses, J. Angeles, and R. Mukherji, Analysis, Optimization, and Testing of Planetary Exploration Rovers: Challenges in Multibody System Modelling, Multibody Dynamics 2013 - ECCOMAS Thematic Conference, Zagreb, (Croatia), 2013.